J. Fluid Mech. (1982), *vol.* 119, *pp.* 107–120
Printed in Great Britain

Boundary conditions at a liquid/air interface in lubrication flows

By K. J. RUSCHAK

Research Laboratories, Eastman Kodak Company, Rochester, New York 14650, U.S.A.

(Received 23 February 1981 and in revised form 26 October 1981)

A difficulty in applying the lubrication approximation to flows where a liquid/air interface forms lies in supplying boundary conditions at the point of formation of the interface that are consistent with the lubrication approximation. The method of matched asymptotic expansions is applied to the flow between partially submerged, counter-rotating rollers, a representative problem from this class, and the lubrication approximation is found to generate the first term of an outer expansion of the problem solution. The first term of an inner expansion describes the two-dimensional flow in the vicinity of the interface, and approximate results are found by the finite-element method. Matching between the inner and outer solutions determines boundary conditions on the pressure and the pressure gradient at the point of formation of the interface which allow the solution to the outer, lubrication flow to be completed.

1. Introduction

There are important applications of the lubrication or Reynolds approximation to flows where a liquid/air interface forms. Cavity formation in a journal bearing is an application of obvious interest. A second notable application is to the various roll-coating devices that are used industrially to form thin liquid films.

As explained, for instance, by Taylor (1963), a difficulty in applying the lubrication approximation to this class of problems lies in providing boundary conditions where the liquid/air interface forms. The lubrication approximation is useful up to the meniscus but not in the immediate vicinity of the meniscus, where the flow is essentially two-dimensional.

Taylor argued that a local analysis for the neighbourhood of the meniscus would resolve the difficulties, but, in view of the apparent intractability of the applicable equations, he resorted instead to special experiments to provide the information he needed. Evidently only Pitts & Greiller (1961) and Coyne & Elrod (1970) have attempted an approximate solution near the meniscus. Both of their approaches involve major simplifying assumptions to make the problem at all tractable. Others have postulated boundary conditions without attempting formal justification. Savage (1977) has critically reviewed some of these proposals. The difficulty with using these boundary conditions lies in identifying the circumstances under which they are valid.

A formal approach is taken here, in the context of the flow between counter-rotating cylinders, which was first studied by Pitts & Greiller (1961). It is first shown that the lubrication approximation arises in the limit as the parameter δ, a measure of the relative slope between the roller surfaces, tends to zero. The fact that these

limiting equations are not applicable throughout the flow field suggests that the parameter limit is singular. The method of matched asymptotic expansions (Van Dyke 1964) is then applicable, and the lubrication approximation is considered to determine the first term of an outer expansion of the problem solution. The co-ordinates are stretched in the neighbourhood of the meniscus, and a second limiting process as $\delta \to 0$ is considered that yields the equations which determine the first term of an inner expansion. The inner problem proves to be intractable, and so it is solved numerically by the finite-element method. Routine matching between the first terms of the outer and inner expansions then produces the boundary conditions that enable the outer solution to be completed.

The use of the method of matched asymptotic expansions leads directly to the boundary conditions for the portion of the flow described by the lubrication approximation. The procedure described is applicable to all the problems in this class, and not just to the particular example used here for illustration.

2. Description of the problem

Two long cylinders of radius R are immersed to their centres in a pool of liquid (figure 1). The axes of the cylinders are parallel, and the minimum gap between the cylinders is $2H_0$. An (X, Y) Cartesian co-ordinate system is oriented as shown in the figure. The cylinders rotate in opposite directions with peripheral speed S, with the effect that a liquid film of uniform thickness is metered onto the surface of each cylinder. The important question of the stability of this flow is not considered here, and the reader may refer to the works of Pitts & Greiller (1961), Mill & South (1967), Savage (1977) and Greener *et al.* (1980).

The liquid has viscosity μ, density ρ and surface tension σ. The pressure is denoted by P, and the X- and Y-components of the velocity by U and V respectively. The Y-co-ordinate of a cylinder surface is given by $F(X)$, where

$$F = H_0 + R - (R^2 - X^2)^{\frac{1}{2}} \quad (|X| \leqslant R). \tag{2.1}$$

The dimensionless parameters for this problem are the Reynolds number $r = \rho S H_0/\mu$, the capillary number $c = \mu S/\sigma$, and what will turn out to be a measure of the relative slope between the cylinder surfaces $\delta = (H_0/R)^{\frac{1}{2}}$.

In the following analysis δ is assumed to be a small parameter. This is not the case in figure 1, where, for clarity, dimensions relative to the cylinder radius have been greatly exaggerated. If the figure were drawn to the scale at which the analysis applies, the cylinders would appear to be touching. Moreover, the thin liquid film on the surface of each cylinder would not be visible, nor would the meniscus, which is very close to the nip.

3. The outer problem

Consider first the portion of the flow in the vicinity of the nip. Scale factors appropriate for this region are well known (Pitts & Greiller 1961) and lead to the following dimensionless variables:

$$x = \delta X/H_0, \quad y = Y/H_0, \quad f = F/H_0; \tag{3.1a,b,c}$$

$$u = U/S, \quad v = V/\delta S, \quad p = \delta H_0 P/\mu S. \tag{3.1d,e,f}$$

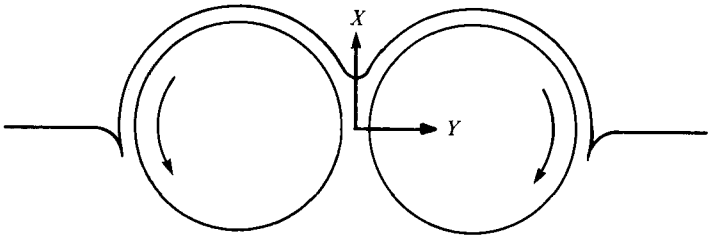

FIGURE 1. Partially submerged, counter-rotating cylinders.

An important point to note is that the scale factor for the X-co-ordinate is much larger than that for the Y-co-ordinate. As a result the streamlines in this region turn out to be nearly parallel.

The governing equations written in terms of these dimensionless variables are as follows:

$$r\delta[uu_x+vu_y] = -p_x+u_{yy}+\delta^2u_{xx}, \tag{3.2a}$$

$$r\delta^3[uv_x+vv_y] = -p_y+\delta^2v_{yy}+\delta^4v_{xx}, \tag{3.2b}$$

$$u_x+v_y = 0, \tag{3.2c}$$

$$u = (1+\delta^2f_x^2)^{-\frac{1}{2}}, \quad v = f_x(1+\delta^2f_x^2)^{-\frac{1}{2}} \quad (y=f), \tag{3.2d,e}$$

$$u_y = 0, \quad v = 0 \quad (y=0), \tag{3.2f,g}$$

$$f = 1+\delta^{-2}-\delta^{-2}(1-\delta^2x^2)^{\frac{1}{2}}. \tag{3.2h}$$

Equations (3.2a,b) are the components of the momentum equation, and (3.2c) is the continuity equation. Boundary conditions (3.2d,e) state that liquid does not slip at the cylinder surfaces. The other two boundary conditions (3.2f,g) express the symmetry of the flow about the x-axis. Finally, (3.2h) is derived from (2.1), and gives the y-co-ordinate of a cylinder surface.

Consider the formal limit of equations (3.2) as $\delta \to 0$ with x and y fixed. The dependent variables u, v, p and f approach limits that, for the sake of simplicity and because higher-order terms will not be calculated, will be designated by the same notation:

$$0 = -p_x+u_{yy}, \quad 0 = -p_y, \tag{3.3a,b}$$

$$u_x+v_y = 0, \tag{3.3c}$$

$$u = 1, \quad v = f_x \quad (y=f), \tag{3.3d,e}$$

$$u_y = 0, \quad v = 0 \quad (y=0), \tag{3.3f,g}$$

$$f = 1+\tfrac{1}{2}x^2. \tag{3.3h}$$

These equations are, in fact, the lubrication approximation to the complete set of equations. Here, they also determine the first term of an outer expansion of the problem solution. They are expected to be valid for small values of δ provided that $r \ll \delta^{-1}$ and $x \ll \delta^{-\frac{1}{2}}$.

From (3.3b) p is a function only of x, and consequently expressions for u, v and p_x follow readily from (3.3):

$$u = 1-\tfrac{1}{2}p_x(f^2-y^2), \tag{3.4a}$$

$$v = \tfrac{1}{2}p_{xx}(f^2y-\tfrac{1}{3}y^3)+p_xff_xy, \tag{3.4b}$$

$$p_x = 3(f-\lambda)/f^3. \tag{3.4c}$$

In (3.4) the unknown constant λ is the flow rate between the centreline and a cylinder surface made dimensionless with SH_0. A change of independent variable transforms the expression for the pressure gradient at (3.4c) into a form that is readily integrated:

$$\tan\theta = x/\sqrt{2} \quad (|\theta| < \tfrac{1}{2}\pi), \tag{3.5}$$

$$p_\theta/3\sqrt{2} = \cos^2\theta - \lambda\cos^4\theta. \tag{3.6}$$

The outer solution is not complete until three constants have been determined. The flow rate λ is unknown, as is m, the value of x where the meniscus forms and the outer solution ceases to be valid. The integration of (3.6) introduces a third constant. Three boundary conditions are needed to determine these constants.

One boundary condition can be arrived at quite readily:

$$p \to 0 \quad (x \to -\infty). \tag{3.7}$$

To obtain this condition, the variables must be rescaled for the pool of liquid. Because the characteristic length in this region of the flow is R, the pressure in the pool will scale with $\mu S/R$. The pressure near the nip, on the other hand, scales with $\mu S/H_0\delta$ (see (3.1f)). Thus the pressure in the pool, compared with the pressure near the nip, is of order δ^3, and a formal application of the method of matched asymptotic expansions to the two regions will lead to (3.7) as a matching condition.

The remaining two boundary conditions are determined in the following sections by rescaling the variables for the neighbourhood of the meniscus, calculating the first term of an inner expansion, and matching the first terms in the inner and outer expansions.

4. The inner problem

In the outer region the streamlines are nearly parallel, leading to the simplified equations (3.3). Near the meniscus, however, the flow is strictly two-dimensional, and those equations are not adequate.

Dimensionless variables that are appropriate for the neighbourhood of the meniscus are as follows:

$$\xi = (X-M)/H_0, \quad y = Y/H_0, \quad h = H/H_0, \quad \bar{f} = F/H_0, \tag{4.1a,b,c,d}$$

$$\bar{u} = U/S, \quad \bar{v} = V/S, \quad \bar{p} = PH_0/\mu S. \tag{4.1e,f,g}$$

$H(X)$ is the Y-co-ordinate of the meniscus, and $M = H_0 m/\delta$ is the value of X for the point on the meniscus that lies on the X-axis. Note from (4.1a) that the X-co-ordinate is shifted so that the origin of the new co-ordinate system is the leading point of the meniscus. The relationships between the inner and outer variables are

$$\xi = (x-m)/\delta, \quad \bar{f} = f, \tag{4.2a,b}$$

$$\bar{u} = u, \quad \bar{v} = \delta v, \quad \bar{p} = p/\delta. \tag{4.2c,d,e}$$

It is clear from (4.2a) that the x-co-ordinate is being stretched in the vicinity of the meniscus.

In terms of the inner variables the governing equations are

$$r(\bar{u}\bar{u}_\xi+\bar{v}\bar{u}_y) = -\bar{p}_\xi+\bar{u}_{yy}+\bar{u}_{\xi\xi}, \tag{4.3a}$$

$$r(\bar{u}\bar{v}_\xi+\bar{v}\bar{v}_y) = -\bar{p}_y+\bar{v}_{yy}+\bar{v}_{\xi\xi}, \tag{4.3b}$$

$$\bar{u}_\xi+\bar{v}_y = 0, \tag{4.3c}$$

$$\left.\begin{aligned} \bar{p}+2\left(\frac{1+h_\xi^2}{1-h_\xi^2}\right)\bar{u}_\xi-\frac{1}{c}\frac{h_{\xi\xi}}{(1+h_\xi^2)^{\frac{3}{2}}} &= 0 \qquad (4.3d)\\ (\bar{u}_y+\bar{v}_\xi)(1-h_\xi^2)-4h_\xi\bar{u}_\xi &= 0 \qquad (4.3e)\\ \bar{v} = h_\xi\bar{u} &\qquad (4.3f) \end{aligned}\right\} \quad (y=h,\ \xi>0),$$

$$h_\xi\to\infty, \quad h\to 0 \quad (\xi\to 0), \tag{4.3g,h}$$

$$h_\xi\to\delta(\delta\xi+m)(1+\delta^2-\delta^2h)^{-1} \quad (\xi\to\infty), \tag{4.3i}$$

$$\left.\begin{aligned} \bar{u}&\to(1+\delta^2z)(1+\bar{f}_\xi^2)^{-\frac{1}{2}} \qquad (4.3j)\\ \bar{v}&\to(1+\delta^2z)\bar{f}_\xi(1+\bar{f}_\xi^2)^{-\frac{1}{2}} \qquad (4.3k) \end{aligned}\right\} \quad (\xi\to\infty,\ 0<z<g),$$

$$g = \delta^{-2}\{[\delta^2(m+\delta\xi)^2+(1+\delta^2-\delta^2h)^2]^{\frac{1}{2}}-1\}, \tag{4.3l}$$

$$\bar{u} = (1+\bar{f}_\xi^2)^{-\frac{1}{2}}, \quad \bar{v} = \bar{f}_\xi(1+\bar{f}_\xi^2)^{-\frac{1}{2}} \quad (y=\bar{f}), \tag{4.3m,n}$$

$$\bar{u}_y = 0, \quad \bar{v} = 0 \quad (y=0,\ \xi<0), \tag{4.3o,p}$$

$$\bar{f} = 1+\delta^{-2}-\delta^{-2}[1-\delta^2(m+\delta\xi)^2]^{\frac{1}{2}}. \tag{4.3q}$$

Equations (4.3*a*, *b*) are the components of the momentum equation, and (4.3*c*) is the continuity equation. Equation (4.3*d*) states that the normal stress exerted by the liquid on the free boundary is balanced by the action of surface tension in the curved meniscus, and (4.3*e*) states that the free boundary supports no tangential stress. The fact that no liquid flows across the free boundary is expressed by (4.3*f*). Boundary conditions (4.3*g*, *h*) result from the symmetry of the meniscus about the ξ-axis, and (4.3*i*) states that the free meniscus is parallel to the cylinder surface far downstream. The liquid film is in rigid-body motion far downstream (4.3*j*, *k*), and the liquid does not slip at the cylinder surface (4.3*m*, *n*). In (4.3*j*)–(4.3*l*), g is the thickness of the liquid layer along the normal to the cylinder surface, and z is a radial co-ordinate measured from the cylinder surface. The fact that the flow is symmetric about the ξ-axis leads to boundary conditions (4.3*o*, *p*). Equation (4.3*q*) gives $\bar{f}$, the y-co-ordinate of the cylinder surface.

The equations that determine the first terms in the inner expansion are found by taking the limit of (4.3) as $\delta\to 0$ with ξ and y fixed. The limits of the dependent variables $\bar{u}, \bar{v}, \bar{p}, h, \bar{f}$ and g will be designated by the same symbols, again for simplicity:

$$r(\bar{u}\bar{u}_\xi+\bar{v}\bar{u}_y) = -\bar{p}_\xi+\bar{u}_{yy}+\bar{u}_{\xi\xi}, \tag{4.4a}$$

$$r(\bar{u}\bar{v}_\xi+\bar{v}\bar{v}_y) = -\bar{p}_y+\bar{v}_{yy}+\bar{v}_{\xi\xi}, \tag{4.4b}$$

$$\bar{u}_\xi+\bar{v}_y = 0, \tag{4.4c}$$

$$\left.\begin{aligned} \bar{p}+2\left(\frac{1+h_\xi^2}{1-h_\xi^2}\right)\bar{u}_\xi-\frac{1}{c}\frac{h_{\xi\xi}}{(1+h_\xi^2)^{\frac{3}{2}}}=0 \quad & (4.4d)\\ (\bar{u}_y+\bar{v}_\xi)(1-h_\xi^2)-4h_\xi\bar{u}_\xi=0 \quad & (4.4e)\\ \bar{v}=h_\xi\bar{u} \quad & (4.4f)\\ h_\xi\to\infty, \quad h\to 0 \quad (\xi\to 0), \quad & (4.4g,h) \end{aligned}\right\} \quad (y=h,\ \xi>0),$$

$$h_\xi\to 0 \quad (\xi\to\infty), \qquad (4.4i)$$

$$\bar{u}\to 1, \quad \bar{v}\to 0 \quad (\xi\to\infty,\ h<y<\bar{f}), \qquad (4.4j,k)$$

$$\bar{u}=1, \quad \bar{v}=0 \quad (y=\bar{f}), \qquad (4.4l,m)$$

$$\bar{u}_y=0, \quad \bar{v}=0 \quad (y=0,\ \xi<0), \qquad (4.4n,o)$$

$$\bar{f}=1+\tfrac{1}{2}m^2. \qquad (4.4p)$$

Equations (4.4) are only valid very close to the point of formation of the meniscus ($\delta\xi \ll m$). They are nearly as complex as (4.3). The only simplification of any importance to have taken place is that in the limit the cylinder surface parallels the centreline at a distance $\bar{f}$ given by (4.4p). This is because, when δ is small, the meniscus forms so close to the nip that the slope of the cylinder surface is small ($f_\xi=\delta m \ll \delta^{\frac{1}{2}}$). Thus, over the small region of the inner flow, the distance of the cylinder surface from the centreline changes very little ($\delta m\xi \ll m^2$).

The problem (4.4) is complete once boundary conditions are specified as $\xi\to-\infty$. These follow when the first terms in the inner and outer expansions are matched by the usual procedure (Van Dyke 1964). It is found that the streamlines in the inner region must become parallel far upstream for matching with the outer flow to be possible:

$$\bar{u}\to 1-\tfrac{3}{2}(1-q)[1-(y/\bar{f})^2], \quad \bar{v}\to 0 \quad (\xi\to-\infty,\ 0<y<\bar{f}). \qquad (4.4q,r)$$

Here the constant q is an unknown, which is determined as part of the solution to the inner problem. It may be interpreted as the flow rate between the centreline and the cylinder surface made dimensionless with $SH_0\bar{f}$, where $\bar{f}$ is given at (4.4p), or as the ratio of the final film thickness to $\bar{f}$. Usually, only two boundary conditions can be associated with the ends of the free boundary, but three conditions (4.4g–i) are posed here. The problem has not been over-specified, however, because the third boundary condition enables q to be determined.

The matching of the first terms of the inner and outer expansions also provides the two boundary conditions that enable the first term of the outer solution to be determined completely:

$$p=0, \quad p_x=3(1-q)/f^2 \quad (x=m). \qquad (4.5a,b)$$

Boundary condition (4.5a), that the pressure in the outer region is zero at the meniscus, results because the pressure has been scaled with viscous forces in both the inner and outer regions. The scale factor for the pressure in the outer region (3.1f) is much larger than the scale factor in the inner region because of the lubrication effect. As a result, pressure changes which occur near the meniscus are relatively unimportant.

Boundary condition (4.5b) states that the pressure gradient in the outer flow, evaluated at the meniscus, must equal the constant pressure gradient of the inner flow

upstream of the meniscus. Equivalently, the parabolic velocity profile of the outer flow (3.4a), evaluated at the meniscus, must be identical to the parabolic velocity profile (4.4q) to which the inner flow tends upstream of the meniscus. Evaluating the pressure gradient in the outer region, (3.4c), at $x = m$ and substituting into (4.5b) gives

$$\lambda = qf \quad (x = m). \tag{4.5c}$$

This alternative form of the second boundary condition states that the flow rates in the inner and outer regions are equal. Until q is determined as part of the solution of the inner problem (4.4), however, (4.5b,c) are not useful.

5. Numerical solution of the inner problem

The inner problem (4.4) is a free boundary problem with the flow field determined by the complete momentum equation. As such, it is intractable, and so a numerical solution by a finite-element method was obtained. A detailed description of the technique used has appeared elsewhere (Ruschak 1980), and consequently only a few introductory remarks will be made here.

An approximate solution to a weak form of the steady Navier–Stokes and continuity equations is constructed by the finite-element method. Working with a weak form of the equations permits the stress boundary conditions on the free boundary to be imposed as natural boundary conditions, a major simplification.

The finite element used is a triangle with nodes at the vertices and midpoints of the sides. The latter nodes are interconnected to form four subtriangles. The approximating function for the pressure is constant in an element, and the components of velocity vary linearly in each subtriangle. Thus the pressure is approximated by a piecewise-constant function, and each velocity component by a piecewise-linear function. The free boundary is also approximated by a piecewise-linear function.

The substitution of the approximating functions for the pressure, velocity components, and the free boundary into the weak form of the momentum and continuity equations gives rise to a set of nonlinear algebraic equations. The algebraic equations are solved simultaneously by a frontal-elimination technique combined with full Newton's iteration. The unknown flow rate q in boundary condition (4.4q) is treated just as any other unknown. No additional iteration loops are required to determine q.

Four finite-element grids were constructed for the present study. The only change made in the problem (4.4) is to multiply the characteristic length scale H_0 by $\bar{f}$ (4.4p) so that the distance between the cylinder surface and the centreline is unity. The upstream portion of one of the grids is shown in figure 2, and table 1 summarizes the prominent features of the grids.

All the grids begin one unit upstream of the tip of the meniscus. Lengthening the grids in the upstream direction does not appreciably change the results. For example, when $r = 0$ and $c = 0{\cdot}2$, grid 1 gives a value for q of 0·217. A grid of comparable density that extends 5 units upstream of the meniscus gives $q = 0{\cdot}216$. This weak upstream influence of the meniscus can be anticipated from the exact, creeping-flow solution of Richardson (1970) for liquid exiting from a slot. The upstream influence becomes even weaker as the Reynolds number is increased.

On the other hand, as will be seen at (5.3), the necessary length of a grid downstream of the meniscus is proportional to the Reynolds number. It is for this reason

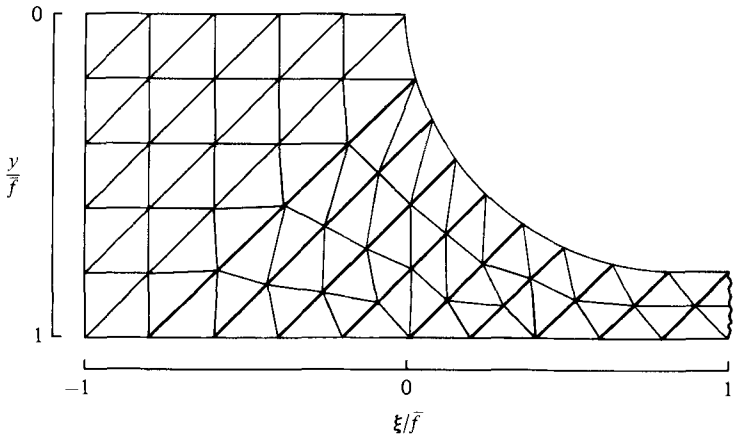

FIGURE 2. Portion of a finite-element grid near the tip of the meniscus. The subtriangles of each element are not shown.

Grid	Nodes	Elements	Unknowns	Length
1	329	136	839	5
2	419	172	1073	9
3	449	192	1147	18
4	415	180	1053	30

TABLE 1. Specifications for the finite-element grids

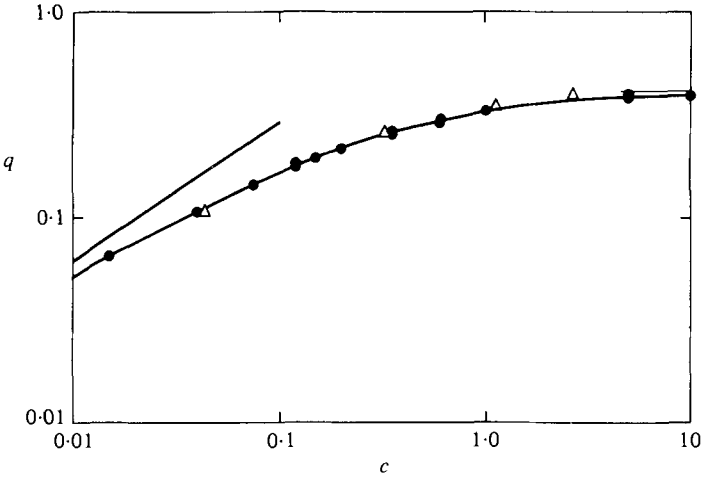

FIGURE 3. Dimensionless flow rate versus the capillary number. ●, present results; △, Coyne & Elrod (1970) for a closely related problem; ——, asymptotic result (5.1) for small capillary number.

that the grids differ in length. Systematic grid refinement was carried out only for the case $r = 0$ and $c = 0{\cdot}2$. Based on the findings, the element densities used are believed to be more than adequate.

The most useful prediction is q, the ratio of the final film thickness to the distance

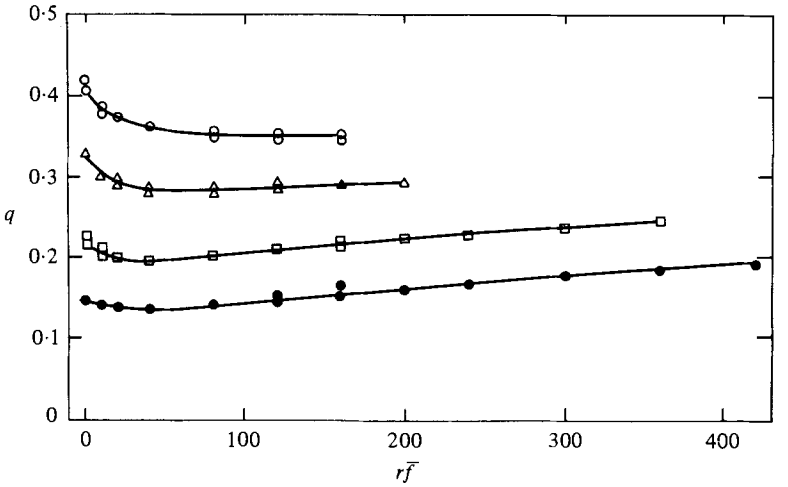

FIGURE 4. Dimensionless flow rate versus the Reynolds number.
○, c = 1000; △, 1; □, 0·2; ●, 0·075.

between the centreline and the cylinder surface. In figure 3 q is plotted against the capillary number for a Reynolds number of zero, as is often effectively the case. The thickness ratio increases monotonically with the capillary number, approaching an upper bound of about 0·41 as the capillary number tends to infinity.

An asymptotic analysis like those performed by Landau & Levich (1942), Bretherton (1961), Ruschak & Scriven (1977), and Ruschak (1977) gives q when the capillary number is small:

$$q \sim 1{\cdot}34c^{\frac{2}{3}} \quad (c \to 0). \tag{5.1}$$

Figure 3, however, shows that this result is of little use for capillary numbers above 0·01. This is expected, however, because a comparison (Ruschak 1974) of (5.1) with Morey's (1940) experimental data at low capillary number shows good agreement only for capillary numbers less than about 0·01.

An approximate result which is somewhat more useful is

$$q = 0{\cdot}54c^{\frac{1}{2}} \quad (0{\cdot}01 < c < 0{\cdot}1). \tag{5.2}$$

Fairbrother & Stubbs (1935) first suggested this form, but with a coefficient of 0·5, based on their experimental results for the thickness of a liquid film deposited in a capillary tube. Taylor (1963) found that his experimental results for a flow geometry similar to that considered here fit the form (5.2), but with a coefficient of 0·43.

Figure 3 also shows the results of the approximate analysis of Coyne & Elrod (1970). The geometry that they considered is very close to that considered here, but the rather good agreement between their results and the present results nevertheless comes as something of a surprise. In constructing their approximate solution, Coyne & Elrod do not even require that the momentum equation be satisfied in some average sense through the liquid, much less at each point.

The thickness ratio was also determined, for several fixed values of the capillary number, as a function of the Reynolds number. Some of these results are shown in figure 4. Perhaps the most noticeable feature of these results is the rather weak

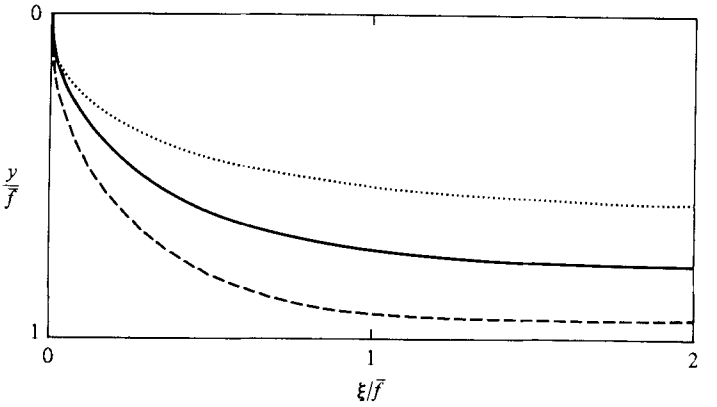

FIGURE 5. Free-boundary profiles at zero Reynolds number. – – –, c = 0·015; ——, 0·2; · · · ·, 1000.

dependence of q on the Reynolds number over the range of the calculations. Another interesting feature of the curves for the lower capillary numbers is that q at first decreases with increasing Reynolds number before beginning a slow but steady increase. Why this should be is not known. The curve corresponding to the highest capillary number appears to approach a lower bound of about $\frac{1}{3}$. This result is reasonable by the following argument. When the Reynolds number is large, the parabolic velocity profile (4.4q) persists up to the tip of the meniscus, where there is a stagnation point. To be consistent with the zero velocity at the stagnation point, the profile must have a zero velocity along the centreline. The parabolic profile (4.4q) meets this condition when q is $\frac{1}{3}$, which is in agreement with the numerical result.

Film profiles at zero Reynolds number are shown in figure 5. In agreement with the findings of Coyne & Elrod (1970), the profiles become flat at a distance downstream which is on the order of one unit. At large Reynolds numbers, however, boundary-layer theory suggests that the distance to a flat profile will be proportional to the Reynolds number. In figure 6 film profiles are plotted for a few Reynolds numbers, the capillary number being 1000. Note that the ξ-co-ordinate has been scaled with the Reynolds number. Plotted in this way, the profiles appear to approach a limit as the Reynolds number becomes large. To support this finding, a very approximate boundary-layer analysis was carried out. The velocity profile across the film was assumed to be parabolic, and the x-component of the momentum equation, reduced to standard boundary-layer form, was satisfied only in the mean across the film. The details will not be given here, as the method is straightforward and there are instances of its application (e.g. Wilkes & Nedderman 1962; Cerro & Scriven 1980; Stucheli & Ozisik 1976). The expression obtained for the film profile is

$$\frac{\xi}{r\bar{f}^2} = \tfrac{1}{30}(Z^2-1)+\tfrac{1}{15}q(Z-1)-\tfrac{1}{18}\ln\frac{Z-q}{1-q}, \tag{5.3}$$

where $Z = 1-h/\bar{f}$ and $q = \sqrt{\frac{1}{6}}$. This approximate result is also plotted in figure 6, and it supports the numerical findings.

In addition to the thickness ratio, the linear extrapolation of the pressure to the tip of the meniscus is also needed later. This was determined by plotting the element

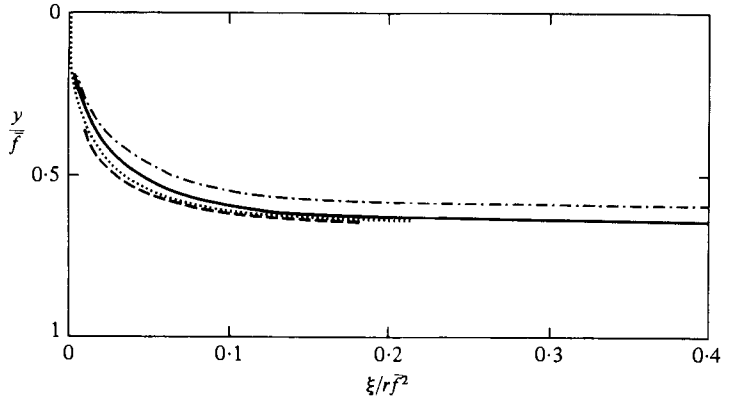

FIGURE 6. Free-boundary profiles for $c = 1000$. ——, $r\bar{f} = 40$; · · · ·, 80; – – –, 160; – · – · – ·, approximate result (5.3).

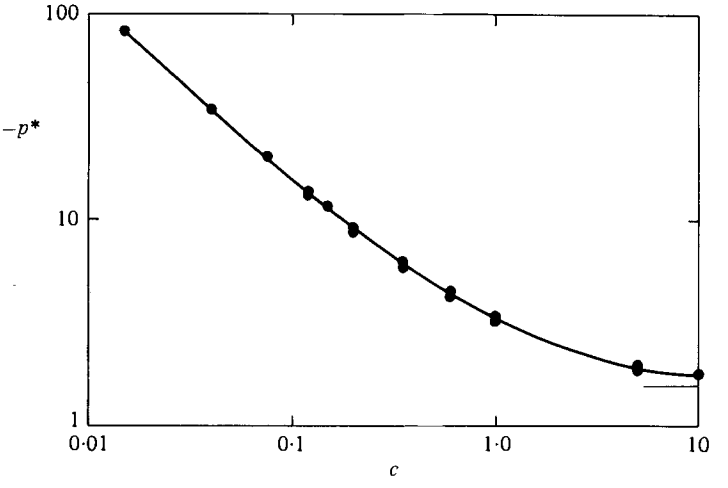

FIGURE 7. Pressure at the meniscus at zero Reynolds number determined by an extrapolation of the constant upstream pressure gradient.

pressures against $\xi/\bar{f}$ for $\xi < 0$. Away from the tip of the meniscus the pressures are independent of y and fall on a straight line with a slope given by

$$\bar{p}_\xi = 3(1-q)/\bar{f}^2. \tag{5.4}$$

The extrapolation of this straight line to $\xi = 0$ gives the desired pressure, which is plotted in figure 7 as a function of the capillary number for a Reynolds number of zero.

6. Completion of the outer solution

The two boundary conditions found by matching, namely (4.5a, c), allow the outer solution to be completed. Written in terms of θ, instead of x (see (3.5)), these boundary conditions are

$$p = 0, \quad q = \lambda \cos^2\theta \quad (\theta = \theta_m), \tag{6.1a, b}$$

where θ_m is the value of θ at $x = m$. With the addition of the third boundary condition (3.7), the differential equation (3.6) for the pressure can now be solved.

First (3.6) is integrated, and (3.7) is used to determine the constant of integration:

$$p/3\sqrt{2} = [\tfrac{1}{4}\pi + \tfrac{1}{2}\theta + \tfrac{1}{4}\sin 2\theta](1 - \tfrac{3}{4}\lambda) - \tfrac{1}{4}\lambda \sin\theta \cos^3\theta. \tag{6.2}$$

Boundary condition (6.1a) is now applied to (6.2):

$$0 = [\tfrac{1}{4}\pi + \tfrac{1}{2}\theta_m + \tfrac{1}{4}\sin 2\theta_m](1 - \tfrac{3}{4}\lambda) - \tfrac{1}{4}\lambda \sin\theta_m \cos^3\theta_m. \tag{6.3}$$

Equations (6.3) and (6.1b) can be solved simultaneously to yield λ and θ_m.

An approximate solution for λ and θ_m is now derived which obviates a numerical solution. Using calculus, it is straightforward to show that the first bracketed term in (6.3) is greater than or equal to $\frac{1}{4}\pi \simeq 0{\cdot}8$ in the interval $(0 \leqslant \theta_m \leqslant \frac{1}{2}\pi)$. Similarly, the coefficient of λ on the far right of (6.3) cannot exceed $3\sqrt{\frac{3}{64}} \simeq 0{\cdot}08$. Thus the first term in (6.3) dominates, and as a result λ must be close to $\frac{4}{3}$. Equation (6.1b) then gives an estimate for θ_m:

$$\lambda \sim \lambda^* = \tfrac{4}{3}, \tag{6.4a}$$

$$\theta_m \sim \theta_m^* = \arccos(\tfrac{3}{4}q)^{\frac{1}{2}}. \tag{6.4b}$$

These first approximations for λ and θ_m can be improved by linearizing (6.1b) and (6.3) about λ^* and θ_m^*. Specifically, the forms

$$\theta_m = \theta_m^* + \theta_m', \tag{6.5a}$$

$$\lambda = \lambda^* + \lambda', \tag{6.5b}$$

where θ_m' and λ' are relatively small quantities, are substituted into (6.1b) and (6.3), and the products of the primed quantities are neglected. The corrections θ_m' and λ' then follow as the solution of two linear equations. The result is

$$\lambda' = \tfrac{8}{3}\theta_m' \tan\theta_m^*, \tag{6.6a}$$

$$\theta_m' = \frac{-\sin\theta_m^* \cos^3\theta_m^*}{3(\theta_m^* + \frac{1}{2}\pi)\tan\theta_m^* + 3 - 4\cos^2\theta_m^* + 2\cos^4\theta_m^*}. \tag{6.6b}$$

The behaviour of the solution is most simply gleaned from (6.4). The approximate location of the meniscus, for instance, follows from (6.4b):

$$m \sim \left[2\left(\frac{4}{3q} - 1\right)\right]^{\frac{1}{2}}. \tag{6.7}$$

As the capillary number increases at a Reynolds number of zero, q increases (figure 3), and consequently m decreases; that is, the meniscus is drawn towards the nip. However, because q never exceeds 0·41, m cannot be less than 2·1, and so the meniscus never reaches the nip.

According to the experimental observations of Pitts & Greiller (1961), there is a region of recirculation just upstream of the meniscus on each side of the centreline, and a stagnation point on the centreline between the meniscus and the nip. Using (3.4a, b) and (6.4a) the position of this stagnation point is found to be $x = \sqrt{6}$. According to (6.7), the meniscus shares this position where $q = \frac{1}{3}$ and hence, from figure 3, $c = 1{\cdot}0$. Thus there are recirculation regions only when $c < 1{\cdot}0$.

7. Concluding remarks

A completely numerical solution to the flow problem could be constructed. This is difficult, however, when δ is small, because the element packing must be dense near the meniscus, and the position of the meniscus varies widely with changes in c and δ. It is far easier in this case to confine the numerical calculations to the vicinity of the meniscus. When the gap between the cylinders is comparable to their radius, however, a completely numerical solution would probably be the best alternative.

As has been discussed, the boundary condition setting the pressure in the outer region to zero at the meniscus (4.5a) results because the pressure has been scaled with viscous forces in both the inner and outer regions. When the capillary number is small, however, the pressure drop across the meniscus is important and the scale factor for the pressure is σ/H_0. Boundary condition (4.5a) would not be accurate under these conditions. The following estimates show that (4.5a) is, however, valid over a large range of capillary number.

The pressure drop across the meniscus is given by p^* (figure 7). Expressed in terms of the outer variable p, this pressure drop is

$$p = \delta \cos^2 \theta_m p^*. \tag{7.1}$$

Using the approximate result (6.4b) for θ_m, (7.1) becomes

$$p = \delta(\tfrac{3}{4} q p^*). \tag{7.2}$$

Since p is of order unity, boundary conditions (4.5a) will be valid when the right-hand side of (7.2) is much less than unity. The results for q and p^* (figures 3 and 7) show that the product p^*q is less than 5·4 when the capillary number is greater than 0·015. Thus, for the right-hand side of (7.2) to be much less than unity for this range of capillary number, it is sufficient that δ is much less than unity, and this is already the case.

When the capillary number is too small, moreover, the flow between the nip and the meniscus cannot, strictly speaking, be described by the lubrication approximation. The position of the meniscus depends on the capillary number through q, and (6.7) and (5.1) show that $m \to \infty$ as $c \to 0$. The outer solution is expected to be valid, however, only when $m \ll \delta^{-\frac{1}{2}}$, which, using (6.7), is equivalent to

$$\delta \ll \tfrac{3}{8} q. \tag{7.3}$$

When this condition is violated, the meniscus forms too far from the nip for the cylinder surfaces to be considered nearly parallel everywhere upstream of the meniscus.

The exact form of the boundary condition on the pressure gradient depends upon the geometry of the problem being considered. In the case of the simple journal bearing studied by Taylor (1963), the boundary condition would be

$$p_x = 6(1 - 2q)/f^2, \tag{7.4}$$

rather than (4.6b). The parameter q would be determined as part of the inner solution for this particular problem. It would be unlikely to differ much from the value of its counterpart in the present problem (figure 3).

Taylor (1963), proceeding largely intuitively, arrived at the correct form for the boundary conditions at the meniscus and proposed essentially the correct local

analysis for the neighbourhood of the meniscus. The application of the method of matched asymptotic expansions clarifies, generalizes and justifies Taylor's results and ideas. The procedure by which boundary conditions can be obtained for any problem in this class is now clear.

REFERENCES

BRETHERTON, F. P. 1961 *J. Fluid Mech.* **10**, 166.

CERRO, R. L. & SCRIVEN, L. E. 1980 *Ind. Engng Chem. Fundam.* **19**, 40.

COYNE, J. C. & ELROD, H. G. 1970 *J. Lub. Tech.* **92**, 451.

FAIRBROTHER, F. & STUBBS, A. E. 1935 *J. Chem. Soc.* 527.

GREENER, J., SULLIVAN, T., TURNER, B. & MIDDLEMAN, S. 1980 *Chem. Engng Commun.* **5**, 73.

LANDAU, L. & LEVICH, B. 1942 *Acta Physicochim. U.S.S.R.* **17**, 42.

MILL, C. C. & SOUTH, G. R. 1967 *J. Fluid Mech.* **28**, 523.

MOREY, F. C. 1940 *Nat. Bur. Standards J. Res.* **25**, 385.

PITTS, E. & GREILLER, J. 1961 *J. Fluid Mech.* **11**, 33.

RICHARDSON, S. 1970 *Rheol. Acta* **9**, 194.

RUSCHAK, K. J. 1974 Ph.D. dissertation, Univ. Minnesota, Minneapolis.

RUSCHAK, K. J. 1977 *Chem. Engng Sci.* **31**, 1057.

RUSCHAK, K. J. 1980 *Int. J. Num. Methods Engng* **15**, 639.

RUSCHAK, K. J. & SCRIVEN, L. E. 1977 *J. Fluid Mech.* **81**, 305.

SAVAGE, M. D. 1977 *J. Fluid Mech.* **80**, 743.

STUCHELI, A. & OZISIK, M. N. 1976 *Chem. Engng Sci.* **31**, 369.

TAYLOR, G. I. 1963 *J. Fluid Mech.* **16**, 595.

VAN DYKE, M. 1964 *Perturbation Methods in Fluid Mechanics.* Academic.

WILKES, J. O. & NEDDERMAN, R. M. 1962 *Chem. Engng Sci.* **17**, 177.